JCTC Journal of Chemical Theory and Computation

Article

pubs.acs.org/JCTC

Accurate Diels–Alder Reaction Energies from Efficient Density Functional Calculations

Pál D. Mezei,[†] Gábor I. Csonka,*[,†] and Mihály Kállay[‡]

[†]Department of Inorganic and Analytical Chemistry, Budapest University of Technology and Economics, H-1521 Budapest, Hungary

[‡]MTA-BME Lendület Quantum Chemistry Research Group, Department of Physical Chemistry and Materials Science, Budapest University of Technology and Economics, H-1521 Budapest, P.O. Box 91, Hungary

Supporting Information

ABSTRACT: We assess the performance of the semilocal PBE functional; its global hybrid variants; the highly parametrized empirical M06-2X and M08-SO; the range separated rCAM-B3LYP and MCY3; the atom-pairwise or nonlocal dispersion corrected semilocal PBE and TPSS; the dispersion corrected range-separated ωB97X-D; the dispersion corrected double hybrids such as PWPB95-D3; the direct random phase approximation, dRPA, with Hartree–Fock, Perdew–Burke–Ernzerhof, and Perdew–Burke–Ernzerhof hybrid reference orbitals and the RPAX2 method based on a Perdew–Burke–Ernzerhof exchange reference orbitals for the Diels–Alder, DARC; and self-interaction error sensitive, SIE11, reaction energy test sets with large, augmented correlation consistent valence basis sets. The dRPA energies for the DARC test set are extrapolated to the complete basis set limit. CCSD(T)/CBS energies were used as a reference. The standard global hybrid functionals show general improvements over the typical endothermic energy error of semilocal functionals, but despite the increased accuracy the precision of the methods increases only slightly, and thus all reaction energies are simply shifted into the exothermic direction. Dispersion corrections give mixed results for the DARC test set. Vydrov–Van Voorhis 10 correction to the reaction energies gives superior quality results compared to the too-small D3 correction. Functionals parametrized for energies of noncovalent interactions like M08-SO give reasonable results without any dispersion correction. The dRPA method that seamlessly and theoretically correctly includes noncovalent interaction energies gives excellent results with properly chosen reference orbitals. As the results for the SIE11 test set and H_2^+ dissociation show that the dRPA methods suffer from delocalization error, good reaction energies for the DARC test set from a given method do not prove that the method is free from delocalization error. The RPAX2 method shows good performance for the DARC, the SIE11 test sets, and for the H_2^+ and H_2 potential energy curves showing no one-electron self-interaction error and reduced static correlation errors at the same time. We also suggest simplified DARC6 and SIE9 test sets for future benchmarking.

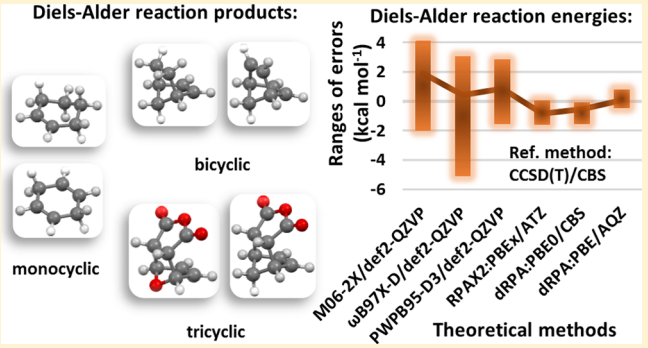

INTRODUCTION

The inexpensive local spin density (LSD) approximation;[1] the semilocal generalized gradient approximation (GGA) density functionals, e.g., PW86,[2] PW91,[3] PBE,[4] and PBEsol;[5] and meta-GGA functionals, e.g., TPSS,[6] revTPSS,[7] and regTPSS,[8] suffer from many-electron self-interaction error (SIE)[9−11] leading to energetic preference for unrealistically delocalized electron densities. Functionals having SIE show particularly large errors for systems with fractional charges,[12,13] as too-delocalized charge distribution leads to too-low energies. For the same reason, SIE overstabilizes the charge transfer complexes, leads to too-low or no reaction energy barriers[14] of chemical reactions, and leads to seriously wrong dissociation energy curves for diatomic cations (e.g., H_2^+).[9] The correct description requires that the ground state total energy $E(N)$ versus number of electrons should be a linkage of straight-line segments connecting the energy values (e.g., $E(N-1)$, $E(N)$, $E(N+1)$) at integer N's.[15] All standard local and semilocal functionals give erroneously smooth convex, almost parabolic energy curves and show no derivative discontinuity at integer electron numbers.[16] Exact exchange has the opposite behavior: it gives the opposite concave energy curve between two integers, due to the missing electron correlation.[16] Mixing the convex and the concave energy curves via hybridization of density functionals might help; however, in practice the popular hybrid functionals still show considerable convexity error.[16] These hybrids can be classified as global (e.g., B3PW91 or B3LYP,[17] PBE0,[18] and TPSSh[19] and variants of BPW91, PBE, and PBEsol hybrids[20]), local (e.g., B05,[21] MCY1,[22] MCY2,[23] and PSTS[24]), or range-separated (e.g., HSE03,[25] ωB97 or ωB97X,[26] MCY3,[27] CAM-B3LYP,[28] or rCAM-B3LYP[27]). The standard global hybrid functionals that mix 20−25% of exact exchange correct only a fraction of the delocalization error (Figure 4 in ref 16) and fail seriously for delocalized stretched odd-electron

Received: March 8, 2015
Published: May 14, 2015

DOI: 10.1021/acs.jctc.5b00223
J. Chem. Theory Comput. 2015, 11, 2879−2888

systems (e.g., dissociating H_2^+). It was found[16] that only MCY3 and rCAM-B3LYP showed signs of improvement in the description of fractional numbers of electrons.

To illustrate the above-discussed SIE or delocalization error, Johnson et al. proposed[16] a test set of 14 representative Diels–Alder reactions. These are the reactions of butadiene, cyclopentadiene, cyclohexadiene, and furane with typical dienophiles as ethene, ethyne, maleic anhydride, and maleimide, as shown in Table 1.

Table 1. Reagents in the 14 Diels–Alder Reactions in the DARC Test Set[a]

no.	reagents	products	
1	ethene + butadiene	monocyclic	
2	ethyne + butadiene		
3	ethene + cyclopentadiene	bicyclic	
4	ethyne + cyclopentadiene		
5	ethene + cyclohexadiene		
6	ethyne + cyclohexadiene		
7	furan + maleic anhydride	(endo)	tricyclic
8	furan + maleic anhydride	(exo)	
9	furan + maleimide	(endo)	
10	furan + maleimide	(exo)	
11	cyclopentadiene + maleic anhydride	(endo)	
12	cyclopentadiene + maleic anhydride	(exo)	
13	cyclopentadiene + maleimide	(endo)	
14	cyclopentadiene + maleimide	(exo)	

[a]Reactions 7–14 lead to tricyclic products with two different endo or exo conformations as noted in parentheses.

This test set is called DARC, and it was included in a larger test set called GMTKN30.[29,30] Inspection of the reactions reveals that intramolecular noncovalent interaction occurs in the larger bicyclic and tricyclic products. Semilocal functionals miss completely the long-range part of the correlation energy, the origin of noncovalent dispersion bonding. And this error cannot be alleviated by the mixing of the exact exchange into the functional as the exact exchange misses completely the electron correlation effects. To include the missing intramolecular attractive dispersion effects, a variety of atom-pairwise dispersion corrections were applied (e.g., DFT-D,[31] DFT-D2,[32] DFT-D3,[33] DFT-D3(BJ),[34] dD10,[35] dDsC,[36] and dDXDM[37]). A different approach is applied by the nonlocal van der Waals density functionals (e.g., vdW-DF-04,[38,39] vdW-DF-10,[40] VV09,[41] and VV10[42]). The Minnesota functionals (e.g., M06L[43] and M11-L[44]) have a flexible meta-GGA form with many parameters to describe main group thermochemistry, kinetics, and noncovalent interactions. Minnesota functionals might improve the medium-range interaction energies; however, they miss the long-range dispersion effects due to exponential decay of the calculated interaction energy with the distance. The Minnesota functionals have several global hybrid variants (e.g., M05,[45] M05-2X,[46] M06, M06-2X,[47] M08-HX, and M08-SO[48]). The global double hybrid functionals (e.g., B2PLYP,[49] DSD-BLYP,[50] and PWPB95[29]) yield improved results for reaction energies. But even these elaborate functionals that include second order perturbation theory require dispersion correction for long-range dispersion effects as in B2PLYP-D3, PWPB95-D3, and DSD-BLYP-D3.

RPA is accurate for noncovalent intra- and intermolecular interactions, and in contrast with the dispersion corrected functionals it captures the nonpairwise-additive nature of the dispersion interactions.[51] It performs moderately for covalent bond rearrangement reactions and gives erroneous short-range correlation and therefore fails seriously for atomization[52] and ionization[53] processes. It also suffers from self-interaction and static correlation error, which lead to the underestimation of barrier heights[54] and to the overestimation of the energy of breaking bonds,[55] respectively. Furthermore, it converges very slowly to the complete basis set limit because the smooth orbital products cannot describe well the electron–electron Coulomb cusps.[56,57]

We also include in this study the SIE11 self-interaction error related test set which exclusively deals with the SIE. It contains 11 reaction energies that are especially sensitive to SIE, including the dissociation energies of five cationic reactions ($M_2^+ \rightarrow M + M^+$, where M = He, H_2O, and NH_3, $C_4H_{10}^+ \rightarrow C_2H_5 + C_2H_5^+$, and $(CH_3)_2CO^+ \rightarrow CH_3 + CH_3CO^+$) and six neutral reactions (ClFCl → ClClF, $C_2H_4\cdots F_2 \rightarrow C_2H_4 + F_2$, benzene···Li → benzene + Li, NaOMg → Na + MgO, and FLiF → Li + F_2). The reference reaction energies were obtained by CCSD(T)/CBS extrapolation. Earlier studies show that many functionals perform relatively poorly for this test set. One of the worst result is given by PBE (cf., Figure 1 in ref 58). The meta-GGA functionals improve over PBE noticeably. Despite its optimization of the parameters, oTPSS gives only a negligible improvement over TPSS, as the many-electron self-interaction error cannot be corrected at the level of semilocal approximation. Among the semilocal functionals, MGGA_MS gives the smallest error.[58] The hybrid functionals perform better, as mixing of exact exchange decreases the electron self-interaction error for exchange, but do not deliver good results. The best performance for the SIE11 test set was observed for the DSD-BLYP-D3 dispersion corrected doubly hybrid functional.[30]

COMPUTATIONAL DETAILS

The exact exchange dependence of the PBE global hybrid functionals was tested using Gaussian 09.[59] For the calculations, we used an efficient triple-ζ basis set called (aug)-cc-pVTZ(-f,-d). It uses the cc-pVTZ(-d) basis set for the hydrogen atoms and the aug-cc-pVTZ(-f) basis set for the heavy atoms. Our PBE reaction energies with this efficient basis are lower approximately by 0.3 kcal mol^{-1} than those with aug-cc-pVTZ (ATZ), and the calculations are considerably faster. The VV10 dispersion corrected density functional results (with ATZ basis set) were obtained with Orca 3.0.1.[60] The DSD-PBEP86 energies (with aug-cc-pVQZ basis set noted as AQZ) were calculated using the Mrcc program,[61] with the D3(BJ) dispersion corrections obtained separately from Orca.[60] The dD10 dispersion corrections (applied on the def2-QZVP energies taken from ref 30) were calculated using our own program. The dRPA, SOSEX, and RPAX2 correlation energies[62] are calculated in the Mrcc program code using the efficient algorithm of Heßelmann.[63] In the Appendix, we give a detailed presentation of these methods. These calculations are very efficient with the ATZ basis set; for example, for one of the largest DARC reaction products (P10), the PBE and TPSS computation times were 5.5 and 7 min, and those of the PBE0, M06-2X, and PWPB95 were 21, 22, and 24 min. The calculation of dispersion corrections took only seconds. The calculation of the dRPA and RPAX2 correlation energies took 10 and 22 min. More details about the efficiency of dRPA can be found in our earlier work.[64]

There are no practical self-consistent dRPA implementations in the density functional framework for single-particle reference orbitals (RO). These calculations are commonly performed in a postprocessing way, where single-particle ROs from a self-consistent

DOI: 10.1021/acs.jctc.5b00223
J. Chem. Theory Comput. 2015, 11, 2879–2888

DFT or HF calculation are used to evaluate both the EX and cRPA terms. Such noniterative density functional calculations are called dRPA@RO or (EX + cRPA)@RO in the literature, where EX + cRPA is an orbital-dependent functional of exact exchange and RPA correlation.[65] In order to distinguish our results yielded by the Ricatti equation with density fitting and Cholesky decomposition, we adopt the nomenclature of dRPA:RO.

We extrapolate the exact exchange and the dRPA correlation energies (see the equations in the Appendix) to the complete basis set (CBS) according to eqs 1 and 2:

$$E_X^{\text{exact}}(\text{CBS}) = E_X^{\text{exact}}(\text{AQZ}) + C_{4,3}^{\text{exact}}(E_X^{\text{exact}}(\text{AQZ}) - E_X^{\text{exact}}(\text{ATZ})) \quad (1)$$

$$E_C^{\text{dRPA:RO}}(\text{CBS}) = E_C^{\text{dRPA:RO}}(\text{AQZ}) + C_{4,3}^{\text{dRPAc:RO}}(E_C^{\text{dRPA:RO}}(\text{AQZ}) - E_C^{\text{dRPA:RO}}(\text{ATZ})) \quad (2)$$

where $C_{4,3}^{\text{exact:HF}} = 0.274$[66] and $C_{4,3}^{\text{dRPA:RO}}$ depends on the choice of the self-consistent reference orbitals. For PBE, PBE0.25, and HF reference orbitals, $C_{4,3}^{\text{dRPAc:PBE}} = 0.856$, $C_{4,3}^{\text{dRPAc:PBE0.25}} = 0.867$, and $C_{4,3}^{\text{dRPAc:HF}} = 0.917$, respectively (for details see ref 67). These values were obtained from a basis set convergence study of the dRPA correlation energies of ethyne and ethene for A*X*Z basis sets with cardinal numbers $X = 3-6$ by finding an optimal α:

$$C_{X,X-1}^{\text{dRPAc:RO}} = \frac{1}{\left(\frac{X}{X-1}\right)^{\alpha} - 1} \quad (3)$$

This corresponds to an inverse power basis set convergence of the $E_C^{\text{dRPA:RO}}$ controlled by α.[68] The CBS(5/4) extrapolations by the H_2^+ and H_2 reference potential energy curves were performed according to eqs 4 and 6 of ref 66 for the HF and CISD correlation energies, respectively.

RESULTS AND DISCUSSION

Inspection of the 14 Diels–Alder reactions in the DARC database reveals that, in the first six reactions, double (ethene) and triple (ethyne) bonds transformed into single and double bonds. The electron delocalization in the dienes is destroyed; moreover in reactions 3–6, bicyclic products are formed. Thus, intramolecular dispersion effects occur compared to the first two reactions where the product is simple monocyclic (cf. Table 1). In the last eight reactions, furane or cyclopentadiene reacts with maleine, and maleimide yields tricyclic products with endo and exo conformations (cf. Table 1). All these features of the products suggest that these reactions require a method that describes the noncovalent intramolecular interactions, the bond multiplicity change, and new bond formation energies correctly. The energetic consequences of the delocalization error (SIE) can be overcompensated by many different factors listed above. In this section, we shall analyze the various error sources and give methods to reliably eliminate those errors.

First, we examine the role of the exact exchange in hybrid functionals. Figure 1 shows the deviations from the reference reaction energies based on CCSD(T)/CBS calculations for PBE and global hybrid PBE0.25, PBE0.32, and PBE0.38 with increasing weight of exact exchange. Table S1 shows the PBE hybrid (aug)-cc-pVTZ(-f,-d) deviations from the benchmark reaction energies. The def2-QZVP results are also presented in Table S1 for comparison. The results in Figure 1 show that increasing the weight of the exact exchange shifts the reaction

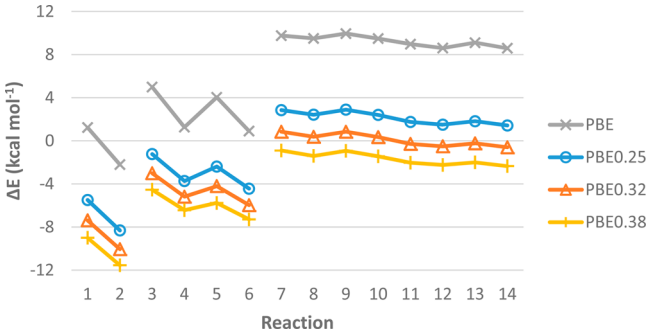

Figure 1. The PBE and global hybrid PBE0.25, PBE0.32,[20] and PBE0.38 deviations from the benchmark reaction energies of the DARC Diels–Alder reaction test set using the (aug)-cc-pVTZ(-f,-d) basis set.

energies in a negative, exothermic direction but does not improve the precision (CSSD) considerably (the tendency is similar for TPSS hybrids in GMTKN30[29] database). Figure 1 shows that PBE gives quite good reaction energies for the first two reactions yielding monocyclic products (cyclohexene and 1,4-cyclohexadiene). However, for reactions leading to bicyclic or tricyclic products, PBE shows a typical DFT error: the reaction energies are erroneously shifted to an endothermic (underbinding) direction. This error is particularly large (more than 8 kcal mol^{-1}) for the tricyclic products (see reactions 7–14 in Figure 1). In these products, the interactions of the bridgehead atoms are intramolecular noncovalent interactions at relatively short distances. The energy errors are related to the tendency of the functionals to overestimate noncovalent repulsion. Johnson et al.[16] supposed that, in the products, there is a region of highly localized electron density that is understabilized by most of the semilocal functionals like PBE in our example.[16] They observed improvement in the calculated reaction energies for functionals with improved treatment of fractionally charged systems. Because of this, they supposed that the errors are related to SIE, the electron delocalization error in DFT, as this error causes semilocal functionals to give too-high energy for localized states or too-low energy for delocalized states. The rCAM-B3LYP and MCY3 functionals, designed to minimize delocalization error, give good results for these reactions (MD = −2.6 and −3.4 kcal mol^{-1} and MAD = 2.6 and 3.4 kcal mol^{-1}, respectively). This logic supposes that the electrons are more localized in the products of the Diels–Alder reactions than in the reactants. Notice that the Diels–Alder reactions are exothermic; thus the large product molecules with an extended electronic system are more stable than the reactants.

Our analysis shows that the self-consistent HF exact exchange electron densities are more compact (localized) than the PBE electron densities in the same molecules with the same nuclear arrangement. Thus, as we increase the weight of the exact exchange in a hybrid functional, we increase the localization of the electron density, and that shifts the reaction energies in the exothermic directions. Thus, the products stabilize more than the reactants. Our results show that we can obtain quite accurate reaction energies using common global PBE hybrid functionals that contain considerable delocalization error. The most accurate is the PBE0.25 hybrid, but the most precise is the PBE0.38 (compare the MD values for accuracy and the CSSD values for precision). The PBE0.32 hybrid yields the best MAD (2.84 kcal mol^{-1}) among these functionals with relatively good accuracy and precision. PBE0.32 hybrid reaction energies are considerably better than those obtained from MCY3 and only slightly worse

DOI: 10.1021/acs.jctc.5b00223
J. Chem. Theory Comput. 2015, 11, 2879–2888

than the rCAM-B3LYP results. In the reactions of ethene, the effect of 25% exact exchange is larger than in the similar reactions of ethyne. The effect of exact exchange is even larger in the reactions of maleic anhydride and maleimide (reaction 7−14 in Figure 1), where the reacting carbon−carbon double bond is a part of a larger conjugated system. Figure 1 shows that the reactions leading to mono-, bi-, and tricyclic products behave quite differently, and the increasing fraction of the exact exchange simply shifts the errors in the exothermic direction.

Next, we discuss the dispersion corrected DFT results. As attractive intramolecular dispersion interactions stabilize the bicyclic and tricyclic products more than the reactants, the calculated dispersion corrected Diels−Alder reaction energy is always shifted in the exothermic direction. Thus, this kind of dispersion correction, the exothermic shift of accurate (small MD) or already exothermic DFT reaction energies, worsens the results (*vide infra* PBE0.32[20] or 38 results). In Figure 2, we show

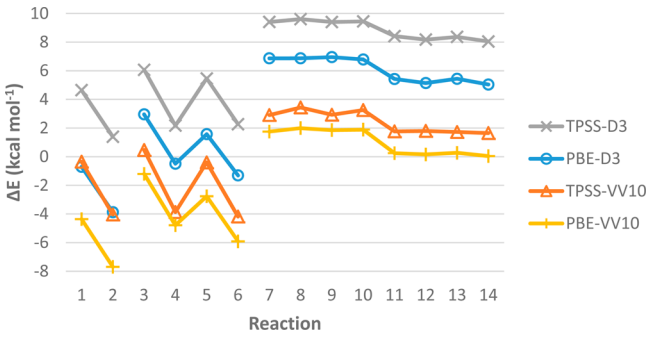

Figure 2. The D3 dispersion corrected (taken from GMTKN30 database[29]) as well as the nonlocal VV10 corrected (this work, using ATZ basis set) PBE and TPSS deviations from the benchmark reaction energies of the DARC Diels−Alder reaction test set.

the deviations of D3 and VV10 corrected PBE and TPSS/ATZ reaction energies from the reference. The energies were taken from the GMTKN30 database.[29] Furthermore, the PBE- and TPSS-D2, -D3, -dD10, and -VV10 deviations from the benchmark reaction energies are presented in Tables S2 and S3 for comparison. The simpler D2 corrected methods seem to be superior to the D3 corrected ones for Diels−Alder reaction energies. The dD10 correction performs similarly to the D2 correction for PBE. The VV10 correction has an even larger effect. Since TPSS is more repulsive than PBE, the corrections are also larger for TPSS than PBE. The dispersion corrected TPSS results are also more precise. These results show that the one-electron self-correlation free TPSS has also a smaller many-electron self-interaction error (cf. SIE11 subset of GMTKN30 database[29]) and this leads to improvements over the dispersion corrected PBE for DARC test set. The dispersion corrected TPSS-dD10 results are even better as MAD = 2.17 kcal mol^{-1}, and the results are quite precise (CSSD = 1.86 kcal mol^{-1}). The VV10 correction for TPSS increases the accuracy of the calculations more than the atom-pairwise corrections.

Figures 1 and 2 show clearly that semilocal functionals yield different errors for reactions with ethene and ethyne, and mixing with exact exchange and applying dispersion correction does not help in this respect. The deviations for the reactions 7−10 or 11−14 are similar because the intramolecular interactions are nearly equal in the cage-like products. In the database, there are many redundant reactions, and the tricyclic reactions are over-represented. Figures 1 and 2 also show that the methods have very similar errors for reactions 7−10 and 11−14. We suggest using a more balanced, smaller database with only six reactions (reactions 1−4, 7, and 11 in Table 1), called DARC6.

Next, we assess the performance of the hybrid functionals that also consider dispersion (Table S4). The dispersion correction shifts the reaction energies in the exothermic direction by stabilizing the products more than the reactants. Consequently, for all methods that reproduce accurately the reaction energies (MD value is around zero) or yield exothermic error (MD value is negative), the accuracy of the dispersion-corrected reaction energies is worsened systematically by 2−4 kcal mol^{-1}. For example, the PBE0.25-D3 results in MD = −3.08 and MAD = 3.13 kcal mol^{-1}, a worsening compared to the PBE0.25 results above. Figure 3 shows the deviations from reference energies for

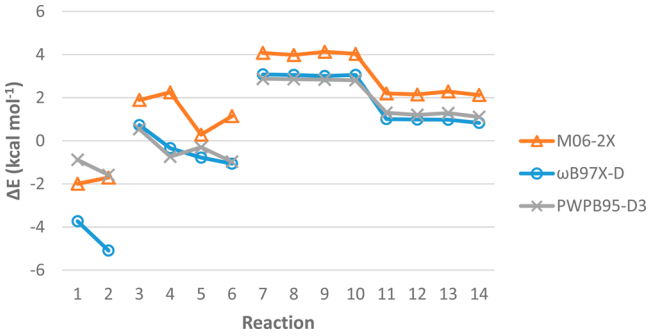

Figure 3. The global hybrid M06-2X, the dispersion corrected range separated hybrid ωB97X-D, and the D3 dispersion corrected global double hybrid PWPB95 (taken from GMTKN30 database[29]) deviations from the benchmark reaction energies of the DARC Diels−Alder reaction test set.

ωB97X-D, M06-2X, and PWPB95-D3 (taken from GMTKN30 database[29]). The dispersion-corrected range-separated hybrid ωB97X-D with 100% of exact exchange in the long range is accurate (MD = 0.41 kcal mol^{-1}) but not precise (CSSD = 2.49 kcal mol^{-1}), leading to MAD = 1.98 kcal mol^{-1}. The M06-2X functional (with 54% of exact exchange) is less accurate (MD = 1.92 kcal mol^{-1}), but it is significantly more precise (CSSD = 1.97 kcal mol^{-1}) than ωB97X-D. Overall, the M06-2X is somewhat worse (MAD= 2.45 kcal mol^{-1}) than ωB97X-D. Somewhat better results can be obtained with the M08-SO functional yielding MD, MAD, and CSSD equal to 0.41, 1.46, and 1.69 kcal mol^{-1}, respectively. The dispersion corrected global double hybrid PWPB95-D3 gives MD, MAD, and CSSD equal to 0.88, 1.52, and 1.59 kcal mol^{-1}, respectively. These latter methods are among the best DFT methods in the literature for the DARC test set.

Finally, we assess the performance of the RPA methods (Tables S5 and S6). dRPA seamlessly integrates dispersion interactions. It can treat chemical reaction energies with good precision, but it contains the SIE. It is interesting how dRPA reproduces these quite complicated bond rearrangements, hybridization changes, and ring formations characteristic to Diels−Alder reactions. It is expected that the intramolecular dispersion effects are well described. *A posteriori* dispersion corrections like D2 or D3 are practical, but several features of such corrections are undesirable, as such corrections are parametrized empirically and might lead to random corrections as it was experienced for anion−π interactions.[64] Even the VV10 correction is pairwise, thus inherently limited. dRPA does not suffer from these problems, and it is very efficiently implemented

DOI: 10.1021/acs.jctc.5b00223
J. Chem. Theory Comput. 2015, 11, 2879−2888

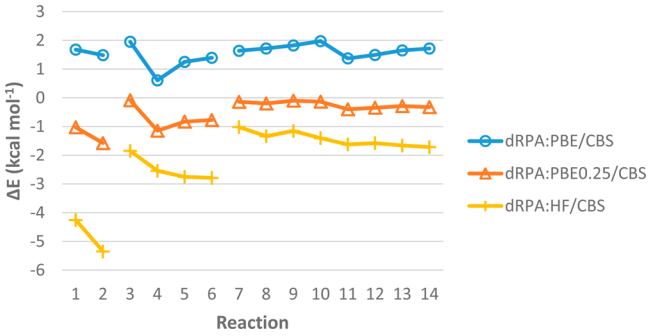

Figure 4. The complete basis set extrapolated dRPA (calculated on self-consistent HF, PBE, PBE0.25 orbitals) deviations from the benchmark reaction energies of the DARC Diels–Alder reaction test set.

in the MRCC program.[61] This makes it possible to calculate CBS extrapolated dRPA energies for such large product molecules included in the DARC test set. In Figure 4, we show dRPA (calculated on self-consistent HF, PBE, and PBE0.25 reference molecular orbitals) deviations from the benchmark Diels–Alder reaction energies. We used CBS extrapolation because dRPA shows slow convergence with respect to the increase of the basis set quality (the ATZ basis set error might shift the calculated dRPA Diels–Alder reaction energies in the exothermic direction by up to 4 kcal mol^{-1}, cf. Table S5). As we discussed above, the HF electron density is more compact than the PBE density, and it causes the exothermic shift in the reaction energies. Consequently using the HF reference orbitals leads to large exothermic error for dRPA:HF/CBS (see also the poorer dRPA:HF/ATZ results in Table S5). The dRPA:PBE/CBS yields a 1.55 kcal mol^{-1} endothermic mean deviation and CSSD = 0.34 kcal mol^{-1}. This is in a good agreement with the results in ref 69, and the origin of the slight difference (0.3 kcal mol^{-1}) is the more refined CBS extrapolation applied in this paper. The dRPA:PBE endothermic error is quite efficiently compensated by the AQZ exothermic basis set error leading to very accurate and precise reaction energies (cf. MD = 0.08, MAD = 0.32, and CSSD = 0.42 kcal mol^{-1} in Table S6). Figure 4 shows the excellent performance of CBS extrapolated dRPA:PBE0.25 (MAD = 0.53 and CSSD = 0.47 kcal mol^{-1}). The RPAX2 method using the ATZ basis set and PBE exchange-only (PBEx) reference orbitals also leads to very precise results with a small exothermic average deviation (MD = −0.83, MAD = 0.83, CSSD = 0.56 kcal mol^{-1}, cf. Table S5). CBS extrapolation of the RPAX2 reaction energies worsens the agreement with the reference reaction energies and leads to small endothermic average deviation (MD = 0.85, MAD = 1.06, CSSD = 0.94 kcal mol^{-1}) as shown in ref 69. The results in ref 69 also show that the application of the SOSEX correction worsens the results (cf. MAD = 2.33 kcal mol^{-1}) as it gives an unbalanced description of the correlation effects within the reactants and products. These errors are properly corrected by the RPAX2 method.[69]

At this point, the question arises of whether the good dRPA:PBE0.25/CBS results for the DARC test set can be related to improved self-correlation error. For this purpose, we use all the SIE11 reference data (kcal mol^{-1}) and the deviations calculated for dRPA:HF, SOSEX:HF, dRPA:PBE, dRPA:PBE0.25, RPAX2:PBEx, PBE0.25, and DSD-BLYP-D3 given in Table 2 along with the statistical analysis of the deviations. All calculations were performed with the ATZ basis set, as the basis set errors are practically negligible compared to the dRPA errors as shown in a separate study. Notice that 10 SIE dissociation reactions in Table 2 are written in the endothermic direction, and only reaction 6 is written in the exothermic direction. The results in Table 2 show that dRPA:HF/ATZ performs quite well for the first five cationic dissociation reactions, while it fails considerably for three neutral dissociation energies of reactions 6 (ClFCl → ClClF), 8 (benzene···Li → benzene + Li), and 11 (FLiF → Li + F_2). The SOSEX:HF/ATZ results are considerably less accurate than the dRPA:HF/ATZ; the MD is shifted by −4 kcal mol^{-1} in the exothermic direction. Replacing the HF reference orbitals by PBE shifts the reaction energies in the endothermic direction (cf. MD = 4.95 kcal mol^{-1} in Table 2), and the precision of the calculations is deteriorated as shown by the large CSSD = 14.44 and MAD = 9.43 kcal mol^{-1} in Table 2. Inspection of the errors in Table 2 reveals that a very large endothermic error (about 43 kcal mol^{-1}) occurs for reaction 11 for dRPA:PBE/ATZ, while errors

Table 2. Reference Reaction Energies Obtained from CCSD(T)/CBS (kcal mol^{-1}), Deviations for Various Calculated Reaction Energies (calculated − reference) and Statistical Data As Mean Deviation, Mean Absolute Deviations, Corrected Sample Standard Deviations, and Minimal and Maximal Deviations for 11 Reactions of SIE11 Test Set[a]

react.	ref. energy	PBE0.25	DSD- BLYP-D3	dRPA: HF	SOSEX: HF	dRPA: PBE	dRPA: PBE0.25	RPAX2: PBEx
1	57.44	12.58	5.68	2.29	−5.82	13.15	9.40	−3.43
2	35.34	6.25	2.24	−2.47	−6.22	4.56	2.57	−1.79
3	37.25	10.99	5.45	−0.95	−7.52	9.81	6.85	−1.07
4	35.28	3.75	0.24	−2.12	−5.68	3.52	2.27	−1.57
5	22.57	7.74	−2.47	−0.87	1.43	0.99	1.43	0.06
6	−1.01	11.48	−1.22	−16.36	−14.89	4.29	1.10	0.80
7	1.08	0.03	−0.07	−0.26	−0.54	−2.86	−0.60	−2.81
8	9.50	−4.09	−7.52	−11.36	−12.61	−10.36	−9.11	−7.24
9	10.50	3.08	1.13	−2.20	−2.43	−2.13	−1.15	−1.54
10	69.56	4.73	−1.36	8.63	13.23	−9.26	−0.76	−6.36
11	94.36	13.31	5.75	11.62	−4.68	42.75	26.46	−6.18
MD		6.35	0.71	−1.28	−4.16	4.95	3.50	−2.83
MAD		**7.09**	**3.01**	**5.38**	**6.82**	**9.43**	**5.61**	**2.98**
CSSD		5.53	4.02	7.82	7.47	14.44	8.95	2.69
Min		−4.09	−7.52	−16.36	−14.89	−10.36	−9.11	−7.24
Max		13.31	5.75	11.62	13.23	42.75	26.46	0.80

[a]All RPA calculations were performed with the ATZ basis set. PBE0.25 and DSD-B3LYP-D3 results are taken from ref 30.

DOI: 10.1021/acs.jctc.5b00223
J. Chem. Theory Comput. 2015, 11, 2879–2888

are considerably smaller for the rest of the reactions. Even using the PBE0.25 hybrid reference yields quite a large (about 26.5 kcal mol^{-1}) error for this reaction, while the results for the other 10 reactions are reasonable, as shown in Table 2. Standard hybrid PBE0.25 results in Table 2 are less accurate but more precise than the dRPA:PBE0.25 results. The RPAX2:PBEx method has medium accuracy but significantly better precision (CSSD = 2.69 kcal mol^{-1}) than the other dRPA methods. The good results for DSD-BLYP-D3 are shown in Table 2, but notice the particularly large errors for reactions 1, 3, 8, and 11. The correct descriptions of reactions 8 and 11 are particularly difficult for the methods presented here. The deviations in Table 2 show that SIE does not manifest well in reaction 7. Notice also that dRPA performs particularly well for reaction 5; consequently the remaining nine reactions (SIE9) would be sufficient to test SIE. We also suggest changing the direction of reaction 6 in order to make all reactions endothermic, this would facilitate the discussion of the endo- or exothermic errors.

Figure 5 shows the dissociation curve of the H_2^+ molecular ion that is the simplest way to present the delocalization error, and it

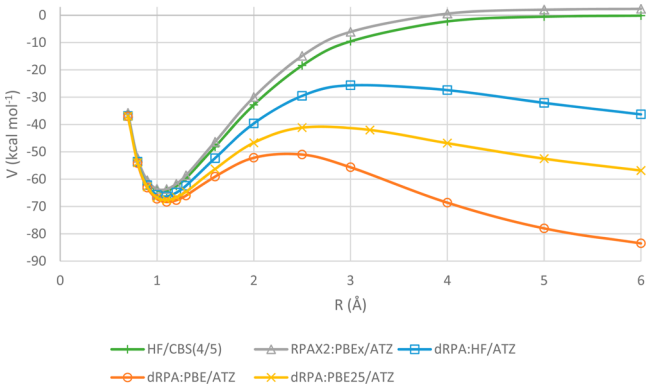

Figure 5. H_2^+ dissociation potential energy curves for RPAX2:PBEx, dRPA:HF, dRPA:PBE, and dRPA:PBE0.25 (all calculations performed with ATZ basis set). The reference curve is calculated from HF/CBS(5/4) with complete basis set extrapolation which uses AQZ and A5Z basis sets.

shows very clearly that all dRPA results suffer from serious one electron SIE, but the magnitude depends on the choice of the reference orbitals. The HF reference leads to considerably better results than the PBE reference, and the PBE0.25 hybrid reference is between them. Thus, the delocalization error increases in the direction of dRPA:HF < dRPA:PBE0.25 < dRPA:PBE. The huge errors above 6 Å are due to the fractional charge problem leading to delocalization error. The dRPA:PBE0.25/ATZ method shows almost 60 kcal mol^{-1} delocalization error at a 6 Å internuclear distance, while it yields excellent performance for the DARC test set. This supports the view that the DARC test set does not really test the delocalization error. The results in Table 3 show that the SIE leads to exothermic error at the equilibrium distance, and the dRPA:HF performs better than dRPA:PBE for the equilibrium distance and bond energy. As expected, the RPAX2 is one-electron self-interaction-free as shown in Table 3 and Figure 5 (the small error of RPAX2 is the consequence of the PBEx reference and the ATZ basis set).

Figure 6 shows the dissociation curve for the H_2 molecule that is the simplest way to present the static correlation error. Notice the large (74 kcal mol^{-1}) error for HF reference orbitals, and the relatively good performance (around 7 kcal mol^{-1} error) for PBE reference orbitals. This also shows that the dRPA error can be

Table 3. Equilibrium Distance (R) and Bond Energy (E) of H_2^+ Molecule Calculated with dRPA:PBE, dRPA:PBE0.25, dRPA:HF, and RPAX2:PBEx Methods Using the ATZ Basis Set[a]

method	R (Å)	E (kcal mol^{-1})
dRPA:PBE	1.11	−68.35
dRPA:PBE0.25	1.09	−67.60
dRPA:HF	1.07	−66.36
RPAX2:PBEx	1.05	−63.90
HF/CBS(5/4)	1.06	−64.40

[a]The reference distance and bond energy is calculated from HF/CBS(5/4) with complete basis set extrapolation, which uses AQZ and A5Z basis sets.

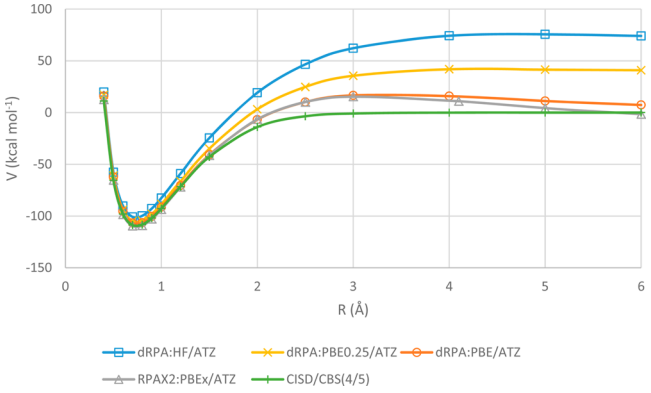

Figure 6. H_2 dissociation potential energy curves for dRPA:HF, dRPA:PBE0.25, dRPA:PBE, and RPAX2:PBEx (all calculations performed with ATZ basis set). The reference curve is calculated from CISD/CBS(5/4) with complete basis set extrapolation, which uses AQZ and A5Z basis sets.

diminished substantially by the proper choice of the reference orbitals. This large improvement can be observed for the equilibrium distance and bond energy calculated with dRPA:PBE shown in Table 4. However, notice the unphysical barrier in

Table 4. Equilibrium Distance (R) and Bond Energy (E) of H_2 Molecule Calculated with dRPA:HF, dRPA:PBE0.25, dRPA:PBE, and RPAX2:PBEx Methods Using the ATZ Basis Set[a]

	R (Å)	E (kcal mol^{-1})
dRPA:HF	0.74	−101.38
dRPA:PBE0.25	0.74	−105.64
dRPA:PBE	0.75	−107.61
RPAX2:PBEx	0.74	−110.42
CISD/CBS(5/4)	0.74	−109.52

[a]The reference distance and bond energy are calculated from CISD/CBS(5/4) with complete basis set extrapolation, which uses AQZ and A5Z basis sets.

Figure 6 for the dRPA:PBE curve. A 25% mixing of exact exchange considerably improves the results compared to the HF reference orbitals leading to 41 kcal mol^{-1} static correlation error. The results in Table 4 show that dRPA:PBE0.25 yields excellent equilibrium geometry and 4 kcal mol^{-1} underbinding error in the dissociation energy. This is an improvement over the 8 kcal mol^{-1} error of the dRPA:HF but worse than the 2 kcal mol^{-1} underbinding error of the dRPA:PBE (cf. Table 4). Inspection of Figure 6 and the results in Table 4 shows the excellent performance of the RPAX2:PBEx method. Notice that the

DOI: 10.1021/acs.jctc.5b00223
J. Chem. Theory Comput. 2015, 11, 2879−2888

dRPAX2 method removes the RPA self-correlation error in third-order.[69]

CONCLUSIONS

In this paper, we assessed the performance of semilocal PBE; global hybrid PBE0.25; PBE0.32; PBE0.38; range-separated hybrid rCAM-B3LYP; MCY3; the D2, D3, dD10, and VV10 dispersion corrected PBE and TPSS; and the M06-2X, M08-SO, ωB97X-D, and PWPB95-D3 as well as the dRPA:HF, dRPA:PBE, dRPA:PBE0.25, and RPAX2:PBEx functionals for the DARC Diels–Alder reaction test set with various basis sets. For PBE and TPSS calculations, we have found that a reduced triple-ζ basis set called (aug)-cc-pVTZ(-f,-d) speeds up the calculations without a significant loss of accuracy. We have found that the energies calculated with semilocal functionals show rapid basis set convergence, and our and literature reaction energies calculated with ATZ or AQZ are practically converged with respect to the basis set extension. This is not true for the dRPA results; thus we performed a complete basis set extrapolation based on the ATZ and AQZ energies. For reference, we used CCSD(T)/CBS reaction energies.

Although the DARC test set was constructed to test the delocalization errors spoiling semilocal DFT results, it is not satisfactorily suitable for that purpose. We have found that it is possible to obtain quite good results for this DARC test set with functionals that contain large delocalization error. This is quite understandable as inspection of the 14 Diels–Alder reactions reveals that in the first six reactions double (ethene) and triple (ethyne) bonds transformed into single and double bonds, the electron delocalization in the dienes is destroyed; moreover bicyclic products are formed with possible intramolecular dispersion effects. In eight reactions, furane or cyclopentadiene reacts with maleine, and maleimide yielding tricyclic products with *endo* and *exo* conformations. Correct energies for these reactions require a method that describes the intramolecular noncovalent bonding, the bond multiplicity change, and formation of new bonds correctly, or systematic multiple error compensation might also lead good results.

We have shown that systematic error compensation is present in PBE hybrids, and the best results can be obtained with mixing 32% exact exchange with 68% PBE exchange (PBE0.32) for the DARC test set. In the PBE0.32 hybrid, the endothermic PBE energy error for reactions leading to bicyclic and tricyclic products is compensated by the exothermic energy error of the exact exchange. This leads to increased average accuracy, but the precision (the corrected sample standard deviation) of the PBE0.32 method does not improve considerably, because the reaction energies are simply shifted in the negative direction. These PBE0.32 results are about the same quality (MAD = 2.8 kcal mol^{-1}) as the results obtained with rCAM-B3LYP and MCY3 with minimal delocalization error (MAD = 2.6 and 3.4 kcal mol^{-1}, respectively), despite the large delocalization error in PBE0.32.

We have shown that *a posteriori* empirical dispersion corrections improve the PBE and TPSS results, by shifting the too-endothermic reaction energies into the exothermic direction. This is because the attractive intramolecular dispersion interactions stabilize the bicyclic and tricyclic products more than the reactants. Consequently, such corrections worsen the already good or too-exothermic reaction energies yielded by PBE hybrids. Our results show that the D2 corrections are better than the D3 corrections, and the D3 corrections are too small. The VV10 corrections are larger and give better results when applicable. We obtained reasonable results with the one-electron self-correlation free TPSS-VV10 functional (MAD = 2.34 kcal mol^{-1}). Minnesota functionals are parametrized to include medium range noncovalent interactions. The M06-2X functional does not show good performance, but the M05-2X and M08-SO functionals give reasonably good agreement with the reference energies (MAD =1.69 and 1.46 kcal mol^{-1}, respectively). The more expensive dispersion corrected global double hybrid PWPB95-D3 gives good agreement with the reference energies (MAD = 1.52 kcal mol^{-1}) with the best precision for this class of functionals.

Direct random phase approximation, dRPA, has many good properties as it seamlessly describes the many-body noncovalent interactions, but it suffers from SIE, thus the delocalization error. We used CBS extrapolated dRPA with HF, PBE, and hybrid PBE0.25 reference orbitals. The too-compact HF electron density leads to more than 2 kcal mol^{-1} exothermic error. The dRPA:PBE and dRPA:PBE0.25 yield excellent results (MAD = 1.55 and 0.53 kcal mol^{-1}, respectively) with much better precision than the best methods discussed above. We have found that dRPA:PBE shows a systematic endothermic error, and that can be compensated by the systematic exothermic error of the AQZ basis set (MAD = 0.32 kcal mol^{-1}). Excellent results can be obtained from RPAX2:PBEx with the ATZ basis set (MAD= 0.83 kcal mol^{-1}) at a considerably higher computational cost compared to dRPA.

Our results show that the DARC test set is not particularly suitable to identify the delocalization error caused by the self-interaction error, but it is an excellent test set for intramolecular interactions. We observed that many reactions in the test sets give the same results; thus by leaving out these calculations, considerable computational effort and time can be saved without the loss of information. We suggest using a reduced DARC6 test set composed of reactions 1, 2, 3, 4, 7, and 11:

no.	reagents	products
1	ethene + butadiene	monocyclic
2	ethyne + butadiene	
3	ethene + cyclopentadiene	bicyclic
4	ethyne + cyclopentadiene	
7	furan + maleic anhydride	tricyclic (endo)
11	cyclopentadiene + maleic anhydride	

The SIE11 test set is more suitable to test the delocalization error than the DARC test set; however, we identified two reaction energies in these sets that are not sensitive to SIE. We observed that it is particularly difficult to obtain good reaction energy for reaction 11 (FLiF → Li + F_2). Only SOSEX:HF and RPAX2:PBEx give reasonable energy for this reaction, while dRPA:PBE gives a very large (around 43 kcal mol^{-1}) endothermic error. Overall, the best results for SIE11 were obtained from the RPAX2:PBEx/ATZ method (MAD = 3 kcal mol^{-1}). We suggest reducing SIE11 to SIE9 by omitting reaction numbesr 5 and 7 and changing the direction of reaction 6.

Inspection of H_2^+ and H_2 dissociation curves reveals that all dRPA methods fail for H_2^+ independent of reference orbitals, and dRPA:PBE performs quite well for H_2 while dRPA:HF fails seriously.

Although the dRPA results presented here are very promising for the DARC test set, the dRPA suffers from serious self-interaction error; thus it yields erroneous dissociation curves and bad atomization energies. A good but more expensive alternative might be the one-electron self-correlation free RPAX2 method

DOI: 10.1021/acs.jctc.5b00223
J. Chem. Theory Comput. 2015, 11, 2879–2888

with lower many-electron self-interaction and static correlation error.

APPENDIX

The general form of the exchange-correlation energy of a global hybrid functional is given by eqs A1 and A2:

$$E_{XC}^{gh} = aE_X^{exact} + (1-a)E_X^{sl} + E_C^{sl} \tag{A1}$$

$$E_X^{exact} = -\frac{1}{2}\sum_{i,j}\langle ij|ji\rangle \tag{A2}$$

where E_X^{exact} is the exact exchange energy calculated from the i and j occupied orbitals (using Dirac's notation). The mixing parameter, a, is equal to 0.25, 0.32, and 0.38 for PBE0.25 (PBE0.25 also called as PBE0 or PBEh in the literature), PBE0.32,[20] and PBE0.38 and 0.10 and 0.25 for TPSS0.1 and TPSS0.25, respectively (TPSS0.1 is called TPSSh and TPSS0.25is called TPSS0 in the literature). E_X^{sl} and E_C^{sl} are the semilocal exchange and correlation energies, respectively.

The atom-pairwise DFT-D2 dispersion correction uses terms depending on the minus sixth power of the interatomic distances (eq A3).

$$E_{disp}^{D2} = -\frac{1}{2}\sum_{i\neq j} s_6 f_{damp}(R_{ij})\frac{C_6^{ij}}{R_{ij}^6} \tag{A3}$$

$$f_{damp}(R_{ij}) = \frac{1}{1+e^{-d\left(\frac{R_{ij}}{R_r}-1\right)}} \tag{A4}$$

where $C_6^{ij} = (C_6^i C_6^j)^{1/2}$, $s_6 = 1.1$ in eq A3, R_r is the sum of atomic van der Waals radii, and $d = 20$ in eq A4.

In addition, the DFT-D3 dispersion correction contains terms depending on the minus sixth and eighth power of the interatomic distances (eq A5).

$$E_{disp}^{D3} = -\frac{1}{2}\sum_{i\neq j}\sum_{n=6,8} s_n f_n(R_{ij})\frac{C_n^{ij}}{R_{ij}^n} \tag{A5}$$

where $s_6 = 1$; s_8 is 0.722, 0.928, 0.998 for PBE, PBE0.25, and PBE0.38 and 1.105, 1.219, and 1.242 for TPSS, TPSS0.1, and TPSS0.25. Each term has a damping function (eq A6), which has a steepness determined by the mean cutoff radius (R_0^{ij}).

$$f_n(R_{ij}) = \frac{1}{1+e^{-d_n\left(\frac{R_{ij}}{s_{r,n}R_0^{ij}}-1\right)}} \tag{A6}$$

The parameters in eq A4 are d_6 =14, d_8 = 16, $s_{r,8} = 1$; $s_{r,6}$ is 1.217, 1.287, 1.333 for PBE, PBE0.25, and PBE0.38 and 1.166, 1.223, and 1.252 for TPSS, TPSS0.1, and TPSS0.25.

With the Becke−Johnson damping function, the correction can be written according to eqs A7 and A8.

$$E_{disp}^{D3(BJ)} = -\frac{1}{2}\sum_{i\neq j}\sum_{n=6,8} s_n\frac{C_n^{ij}}{R_{ij}^n + f^n(R_0^{ij})} \tag{A7}$$

$$f(R_0^{ij}) = a_1 R_0^{ij} + a_2 \tag{A8}$$

where $R_0^{ij} = (C_8^{ij}/C_6^{ij})^{1/2}$, the global scaling factors of the energy terms are $\{s_6, s_8\} = \{0.418, 0.0\}$ for PBEP86, while the parameters in the Becke−Johnson damping are $\{a_1, a_2\} = \{0.0, 5.65\}$ for PBEP86.

The dD10 dispersion correction is also an atom-pairwise correction but contains also terms depending on the tenth power of the interatomic distances and double damping.

$$E_{disp}^{dD10} = -\frac{1}{2}\sum_{i\neq j} F_d(a, R_{ij})\sum_{n=3}^{5} f_{2n}(b\cdot R_{ij})\frac{C_{2n}^{ij}}{R_{ij}^{2n}} \tag{A9}$$

The Fermi damping is given by eq A10, and the mean van der Waals radius is given by

$$R_{ij}^{vdW} = \frac{R_{i,vdW}^3 + R_{j,vdW}^3}{R_{i,vdW}^2 + R_{j,vdW}^2}$$

$$F_d(a, R_{ij}) = 0.5\cdot\left\{1 + th\left[23\cdot\left(\frac{R_{ij}}{a\cdot R_{ij}^{vdW}} - 1\right)\right]\right\} \tag{A10}$$

The atomic van der Waals radii are $R_{vdw}^H = 1.2$ Å, $R_{vdw}^C = 1.7$ Å, $R_{vdw}^N = 1.55$ Å, and $R_{vdw}^O = 1.52$ Å. The parameter of the Fermi damping function is a global constant ($a = 1.45$). The individual damping function of each term is given by eq A11.

$$f_{2n}(b\cdot R_{ij}) = 1 - e^{-b\cdot R_{ij}}\sum_{k=0}^{2n}\frac{(b\cdot R_{ij})^k}{k!} \tag{A11}$$

The parameter of the individual damping functions depends on the choice of density functional ($b = 1.11$ for PBE and $b = 1.8$ for TPSS) fitted to the S22 database. We slightly modified the original method using the C_6 coefficient for any type of i−j atom pairs given by

$$C_6^{ij} = \frac{2\cdot C_6^i\cdot C_6^j}{C_6^i\cdot\frac{\alpha_0^j}{\alpha_0^i} + C_6^j\cdot\frac{\alpha_0^i}{\alpha_0^j}} \tag{A12}$$

where $C_6^H = 2.845$, $C_6^C = 26.36$, $C_6^N = 19.48$, $C_6^O = 12.415$,[70] $\alpha_0^H = 2.75$, $\alpha_0^C = 8.64$, $\alpha_0^N = 7.4$, and $\alpha_0^O = 5.4$.[71] The C_8 and C_{10} coefficients can be estimated as $C_8^{ij} \approx 10\cdot(C_6^{ij})^{0.25}$ and $C_{10}^{ij} \approx 121\cdot(C_6^{ij})^{0.5}$.

The nonlocal VV10 dispersion correction has a form given by eq A13.

$$E_C^{VV10}[n(\vec{r})] = \frac{1}{2}\iint n(\vec{r})\,\Phi(\vec{r},\vec{r}')\,n(\vec{r}')\,d^3\vec{r}\,d^3\vec{r}' - \int\varepsilon_C^{nl,unif}[n(\vec{r})]n(\vec{r})\,d^3\vec{r} \tag{A13}$$

The first term is a two electron integral with the $\Phi(\vec{r},\vec{r}')$ interaction kernel (eq A14), the second term assures that the correction vanishes at uniform electron density.

$$\Phi(\vec{r},\vec{r}') = -\frac{3}{2}\frac{1}{g(\vec{r})\,g(\vec{r}')(g(\vec{r})+g(\vec{r}'))} \tag{A14}$$

where $g(\vec{r}) = \omega_0(\vec{r})R^2 + \kappa(\vec{r})$ with $R = |\vec{r}-\vec{r}'|$ distance and $\omega_0(\vec{r}) = (\omega_1^2(\vec{r}) + \omega_G^2(\vec{r}))^{1/2}$ local frequency. The local dipole resonance frequency $\omega_1(\vec{r}) = 3^{-1/2}\omega_P(\vec{r})$ is computed from the local plasma frequency: $\omega_P(\vec{r}) = (4\pi n(\vec{r}))^{1/2}$. The local band gap is approximated by $\omega_G(\vec{r}) = \sqrt{C|(\nabla n(\vec{r})/n(\vec{r}))|^2}$ where $C = 0.0093$. The second term of $g(\vec{r})$ can be expressed as $\kappa(\vec{r}) = B(\nu_F^2(\vec{r})/\omega_P(\vec{r}))$ where $\nu_F(\vec{r}) = (3\pi^2 n(\vec{r}))^{1/3}$ is the local Fermi velocity. The parameter B is 5.0, 5.4, 6.2, and 6.5 for TPSS, TPSS0.1, PBE, and PBE0.25, respectively.

The general form of the global double hybrid exchange-correlation functionals is given by eq A15.

$$E_{XC}^{gdh} = a_X E_X^{exact} + (1-a_X)E_X^{sl} + a_C E_C^{PT2} + (1-a_C)E_C^{sl} \tag{A15}$$

DOI: 10.1021/acs.jctc.5b00223
J. Chem. Theory Comput. 2015, 11, 2879−2888

where E_C^{PT2} is the second-order perturbation correlation given by eq A16. The parameters in eq A14 are $a_X = 0.53$ and $a_C = 0.27$ for B2PLYP ($a_S = 1$, $a_T = 1$ in eq A16). For DSD-BLYP, the parameters are $a_X = 0.69$ and $a_C = 0.54$ with scaling down the same-spin PT2 component to 80% ($a_S = 1$, $a_T = 0.8$ in eq A16). For PWPB95, the parameters are $a_X = 0.50$ and $a_C = 0.269$ with only the opposite-spin PT2 component ($a_S = 1$, $a_T = 0$ in eq A16).

$$E_C^{PT2} = a_S E_S^{PT2} + a_T E_T^{PT2} \tag{A16}$$

where the spin components are given by eqs A17 and A18 with the pair energies (eqs A19, A20, and A21) and the amplitudes (eq A22) using Dirac's notation for the integrals.

$$E_S^{PT2} = \sum_{i_\alpha j_\beta} e_{i_\alpha j_\beta} \tag{A17}$$

$$E_T^{PT2} = \frac{1}{2}\sum_{i_\alpha j_\alpha} e_{i_\alpha j_\alpha} + \frac{1}{2}\sum_{i_\beta j_\beta} e_{i_\beta j_\beta} \tag{A18}$$

$$e_{i_\alpha j_\beta} = \sum_{a_\alpha b_\beta} T_{i_\alpha j_\beta}^{a_\alpha b_\beta} \langle i_\alpha j_\beta | a_\alpha b_\beta \rangle \tag{A19}$$

$$e_{i_\alpha j_\alpha} = \sum_{a_\alpha b_\alpha} (T_{i_\alpha j_\alpha}^{a_\alpha b_\alpha} - T_{i_\alpha j_\alpha}^{b_\alpha a_\alpha}) \langle i_\alpha j_\alpha | a_\alpha b_\alpha \rangle \tag{A20}$$

$$e_{i_\beta j_\beta} = \sum_{a_\beta b_\beta} (T_{i_\beta j_\beta}^{a_\beta b_\beta} - T_{i_\beta j_\beta}^{b_\beta a_\beta}) \langle i_\beta j_\beta | a_\beta b_\beta \rangle \tag{A21}$$

and

$$T_{i_\alpha j_\beta}^{a_\alpha b_\beta} = \frac{\langle i_\alpha j_\beta | a_\alpha b_\beta \rangle}{\varepsilon_{i_\alpha} + \varepsilon_{j_\beta} - \varepsilon_{a_\alpha} - \varepsilon_{b_\beta}} \tag{A22}$$

The i and j indices belong to the occupied orbitals. The a and b indices belong to the virtual orbitals. α and β are spin indices. The energy of the ith orbital is ε_{i_α} etc. $T_{i_\alpha j_\beta}^{a_\alpha b_\beta}$ are the double excitation amplitude matrix elements. The DFT-D3 parameters $\{s_6, s_{r,8}, s_8\}$ are $\{0.64, 1.427, 1.022\}$ for B2PLYP, $\{0.50, 1.569, 0.705\}$ for DSD-BLYP, and $\{0.82, 1.557, 0.705\}$ for PWPB95.

The direct random phase approximation (dRPA) exchange-correlation energy is given by eq A23.

$$E_{XC}^{dRPA} = E_X^{exact} + E_C^{dRPA} \tag{A23}$$

where the dRPA correlation is given by eq A24. The exact exchange (eq 2) and dRPA correlation energies are generally calculated on self-consistent HF, PBE, or PBE0.25 orbitals.

$$E_c^{dRPA} = \frac{1}{2} tr[\mathbf{BT}] \tag{A24}$$

$$B_{ia,jb} = \langle ij | ab \rangle \tag{A25}$$

where $\mathbf{B}$ is the non-antisymmetrized two-electron repulsion integral matrix (eq A25) and $\mathbf{T}$ is double excitation amplitude matrix given by the iterative update (the iteration is initialized with $\mathbf{T}^{(0)} = \mathbf{0}$) according to eq A26 with the Hadamard product of Δ defined by eq A27.

$$\mathbf{T}^{(n+1)} = -\Delta \circ (\mathbf{B} + \mathbf{B}\mathbf{T}^{(n)} + \mathbf{T}^{(n)}\mathbf{B} + \mathbf{T}^{(n)}\mathbf{B}\mathbf{T}^{(n)}) \tag{A26}$$

$$\Delta_{ia,jb} = \frac{1}{\epsilon_a + \epsilon_b - \epsilon_i - \epsilon_j} \tag{A27}$$

The equations are solved in an $O(n^4)$-scaling iterative procedure with the density-fitted form of electron repulsion integrals and the Cholesky decomposition of matrix Δ.[62]

The dRPA + SOSEX (we use SOSEX for short) correlation energy is obtained as

$$E_c^{SOSEX} = \frac{1}{2} tr[\mathbf{KT}] \tag{A28}$$

where $K_{ia,jb} = \langle ij \| ab \rangle$ are spin-singlet adapted antisymmetrized two electron repulsion integrals.

The RPAX2 correlation energy is defined by eq A29 with the density-fitted form of matrix $\mathbf{B}$ according to eq A30.

$$E_c^{RPAX2} = \frac{1}{2} tr[\mathbf{L}^T \mathbf{T}^{(\infty)} \mathbf{L}] \tag{A29}$$

$$\mathbf{B} = \mathbf{L}\mathbf{L}^T \tag{A30}$$

The iteration is initialized with $\mathbf{T}^{(0)} = \mathbf{0}$; then the amplitudes of the iteration cycles are given by

$$\mathbf{T}^{(n+1)} = -\Delta \circ [(\mathbf{1} + \mathbf{T}^{(n)})\mathbf{B}(\mathbf{1} + \mathbf{T}^{(n)}) - \hat{P}(\mathbf{1} + \mathbf{T}^{(n)})\mathbf{B}(\mathbf{1} + \mathbf{T}^{(n)})] \tag{A31}$$

where $\hat{P}$ is a permutation operator that permutes the orbitals. Δ is decomposed using the Cholesky decomposition. The equations are solved in an $O(n^5)$-scaling iterative procedure.

■ ASSOCIATED CONTENT

Supporting Information

Six tables show the deviations from the reference Diels–Alder reaction energies and statistics for several methods discussed in this paper. The Supporting Information is available free of charge on the ACS Publications website at DOI: 10.1021/acs.jctc.5b00223.

■ AUTHOR INFORMATION

Corresponding Author

*E-mail: csonkagi@gmail.com.

Notes

The authors declare no competing financial interest.

■ ACKNOWLEDGMENTS

G.I.C. acknowledges the support by the New Hungary Development Plan (Project ID: TAMOP- 4.2.1/B-09/1/KMR-2010-0002) at the BME project. The authors thank for the Hungarian National higher education and research network for the computer time.

■ REFERENCES

(1) Kohn, W.; Sham, L. J. *Phys. Rev.* **1965**, *140*, A1133.
(2) Perdew, J. P.; Wang, Y. *Phys. Rev. B* **1986**, *33*, 8800–8802.
(3) Perdew, J. P. In *Electronic Structure of Solids '91*; Ziesche, P., Eschrig, H., Eds.; Akademie Verlag: Berlin, 1991; p 11.
(4) Perdew, J.; Burke, K.; Ernzerhof, M. *Phys. Rev. Lett.* **1996**, *77*, 3865–3868.
(5) Ruzsinszky, A.; Csonka, G. I.; Scuseria, G. E. *J. Chem. Theory Comput.* **2009**, *5*, 763–769.
(6) Tao, J.; Perdew, J. P.; Staroverov, V. N.; Scuseria, G. E. *Phys. Rev. Lett.* **2003**, *91*, 146401.
(7) Perdew, J. P.; Ruzsinszky, A.; Csonka, I.; Constantin, L. A.; Sun, J. *Phys. Rev. Lett.* **2009**, *103*, 026403.
(8) Ruzsinszky, A.; Sun, J.; Xiao, B.; Csonka, G. I. *J. Chem. Theory Comput.* **2012**, *8*, 2078–2087.
(9) Perdew, J. P.; Zunger, A. *Phys. Rev. B* **1981**, *23*, 5048–5079.

DOI: 10.1021/acs.jctc.5b00223
J. Chem. Theory Comput. 2015, 11, 2879–2888

(10) Cohen, A. J.; Mori-Sánchez, P.; Yang, W. *Science* **2008**, *321*, 792−794.
(11) Ruzsinszky, A.; Perdew, J. P.; Csonka, G. I.; Vydrov, O. A; Scuseria, G. E. *J. Chem. Phys.* **2007**, *126*, 104102.
(12) Ruzsinszky, A.; Perdew, J. P.; Csonka, G. I.; Vydrov, O. A; Scuseria, G. E. *J. Chem. Phys.* **2006**, *125*, 194112.
(13) Ruzsinszky, A.; Perdew, J. P.; Csonka, G. I.; Scuseria, G. E.; Vydrov, O. A. *Phys. Rev. A* **2008**, *77*, 060502.
(14) Csonka, G. I.; Johnson, B. G. *Theor. Chim. Act.* **1998**, *99*, 158−165 and references cited therein.
(15) Perdew, J. P.; Levy, M.; Balduz, J. L. *Phys. Rev. Lett.* **1982**, *49*, 1691−1694.
(16) Johnson, E. R.; Mori-Sánchez, P.; Cohen, A. J.; Yang, W. *J. Chem. Phys.* **2008**, *129*, 204112.
(17) Becke, A. D. *J. Chem. Phys.* **1993**, *98*, 5648−5652.
(18) Adamo, C.; Barone, V. *J. Chem. Phys.* **1999**, *110*, 6158.
(19) Staroverov, V. N.; Scuseria, G. E.; Tao, J.; Perdew, J. P. *J. Chem. Phys.* **2003**, *119*, 12129.
(20) Csonka, G. I.; Perdew, J. P.; Ruzsinszky, A. *J. Chem. Theory Comput.* **2010**, *6*, 3688−3703.
(21) Becke, A. D. *J. Chem. Phys.* **2005**, *122*, 064101.
(22) Mori-Sánchez, P.; Cohen, A. J.; Yang, W. *J. Chem. Phys.* **2006**, *124*, 091102.
(23) Cohen, A. J.; Mori-Sánchez, P.; Yang, W. *J. Chem. Phys.* **2007**, *127*, 034101.
(24) Perdew, J. P.; Staroverov, V. N.; Tao, J.; Scuseria, G. E. *Phys. Rev. A* **2008**, *78*, 14.
(25) Heyd, J.; Scuseria, G. E.; Ernzerhof, M. *J. Chem. Phys.* **2003**, *118*, 8207.
(26) Chai, J. D.; Head-Gordon, M. *J. Chem. Phys.* **2008**, *128*, 084106.
(27) Cohen, A. J.; Mori-Sánchez, P.; Yang, W. *J. Chem. Phys.* **2007**, *126*, 191109.
(28) Yanai, T.; Tew, D. P.; Handy, N. C. *Chem. Phys. Lett.* **2004**, *393*, 51−57.
(29) Goerigk, L.; Grimme, S. *J. Chem. Theory Comput.* **2011**, *7*, 291−309.
(30) Goerigk, L.; Grimme, S. *Phys. Chem. Chem. Phys.* **2011**, *13*, 6670−6688.
(31) Grimme, S. *J. Comput. Chem.* **2004**, *25*, 1463−1473.
(32) Grimme, S. *J. Comput. Chem.* **2006**, *27*, 1787−1799.
(33) Grimme, S.; Antony, J.; Ehrlich, S.; Krieg, H. *J. Chem. Phys.* **2010**, *132*, 154104.
(34) Grimme, S.; Ehrlich, S.; Goerigk, L. *J. Comput. Chem.* **2011**, *32*, 1456−1465.
(35) Steinmann, S. N.; Csonka, G.; Corminboef, C. *J. Chem. Theory Comput.* **2009**, *5*, 2950−2958.
(36) Steinmann, S. N.; Corminboeuf, C. *J. Chem. Theory Comput.* **2011**, *7*, 3567−3577.
(37) Steinmann, S. N.; Wodrich, M. D.; Corminboeuf, C. *Theor. Chem. Acc.* **2010**, *127*, 429−442.
(38) Dion, M.; Rydberg, H.; Schröder, E.; Langreth, D. C.; Lundqvist, B. I. *Phys. Rev. Lett.* **2004**, *92*, 246401.
(39) Dion, M.; Rydberg, H.; Schröder, E.; Langreth, D.; Lundqvist, B. *Phys. Rev. Lett.* **2005**, *95*, 109902.
(40) Lee, K.; Murray, É. D.; Kong, L.; Lundqvist, B. I.; Langreth, D. C. *Phys. Rev. B* **2010**, *82*, 081101.
(41) Vydrov, O.; Van Voorhis, T. *Phys. Rev. Lett.* **2009**, *103*, 063004.
(42) Vydrov, O.; Van Voorhis, T. *J. Chem. Phys.* **2010**, *133*, 244103.
(43) Zhao, Y.; Truhlar, D. G. *J. Chem. Phys.* **2006**, *125*, 194101.
(44) Peverati, R.; Truhlar, D. G. *J. Phys. Chem. Lett.* **2012**, *3*, 117−124.
(45) Zhao, Y.; Schultz, N. E.; Truhlar, D. G. *J. Chem. Phys.* **2005**, *123*, 1−4.
(46) Zhao, Y.; Schultz, N.; Truhlar, D. G. *J. Chem. Theory Comput.* **2006**, *2*, 364.
(47) Zhao, Y.; Truhlar, D. G. *Theor. Chem. Acc.* **2007**, *120*, 215−241.
(48) Zhao, Y.; Truhlar, D. G. *J. Chem. Theory Comput.* **2008**, *4*, 1849.
(49) Grimme, S. *J. Chem. Phys.* **2006**, *124*, 034108.
(50) Kozuch, S.; Gruzman, D.; Martin, J. M. L. *J. Phys. Chem. C* **2010**, *114*, 20801−20808.
(51) Eshuis, H.; Furche, F. *J. Phys. Chem. Lett.* **2011**, *2*, 983−989.
(52) Furche, F. *Phys. Rev. B* **2001**, *64*, 195120.
(53) Jiang, H.; Engel, E. *J. Chem. Phys.* **2007**, *127*, 1−11.
(54) Paier, J.; Ren, X.; Rinke, P.; Scuseria, G. E.; Grüneis, A.; Kresse, G.; Scheffler, M. *New J. Phys.* **2012**, *14*, 043002.
(55) Henderson, T. M.; Scuseria, G. E. *Mol. Phys.* **2010**, *108*, 2511−2517.
(56) Noga, J.; Kutzelnigg, W.; Klopper, W. *Chem. Phys. Lett.* **1992**, *199*, 497−504.
(57) Tew, D. P.; Klopper, W.; Helgaker, T. *J. Comput. Chem.* **2007**, *28*, 1307−1320.
(58) Hao, P.; Sun, J.; Xiao, B.; Ruzsinszky, A.; Csonka, G. I.; Tao, J.; Glindmeyer, S.; Perdew, J. P. *J. Chem. Theory Comput.* **2013**, *9*, 355−363.
(59) Frisch, M. J.; Trucks, G. W.; Schlegel, H. B.; Scuseria, G. E.; Robb, M. A.; Cheeseman, J. R.; Scalmani, G.; Barone, V.; Mennucci, B.; Petersson, G. A.; Nakatsuji, H.; Caricato, M.; Li, X.; Hratchian, H. P.; Izmaylov, A. F.; Bloino, J.; Zheng, G.; Sonnenberg, J. L.; Hada, M.; Ehara, M.; Toyota, K.; Fukuda, R.; Hasegawa, J.; Ishida, M.; Nakajima, T.; Honda, Y.; Kitao, O.; Nakai, H.; Vreven, T.; Montgomery, J. A., Jr.; Peralta, J. E.; Ogliaro, F.; Bearpark, M.; Heyd, J. J.; Brothers, E.; Kudin, K. N.; Staroverov, V. N.; Kobayashi, R.; Normand, J.; Raghavachari, K.; Rendell, A.; Burant, J. C.; Iyengar, S. S.; Tomasi, J.; Cossi, M.; Rega, N.; Millam, J. M.; Klene, M.; Knox, J. E.; Cross, J. B.; Bakken, V.; Adamo, C.; Jaramillo, J.; Gomperts, R.; Stratmann, R. E.; Yazyev, O.; Austin, A. J.; Cammi, R.; Pomelli, C.; Ochterski, J. W.; Martin, R. L.; Morokuma, K.; Zakrzewski, V. G.; Voth, G. A.; Salvador, P.; Dannenberg, J. J.; Dapprich, S.; Daniels, A. D.; Farkas, Ö.; Foresman, J. B.; Ortiz, J. V.; Cioslowski, J.; Fox, D. J. *Gaussian 09*, Revision C.01; Gaussian, Inc.: Wallingford, CT, 2009.
(60) Neese, F. *Wiley Interdiscip. Rev.: Comput. Mol. Sci.* **2012**, *2*, 73−78.
(61) MRCC, a quantum chemical program suite written by M. Kállay, Z. Rolik, I. Ladjánszki, L. Szegedy, B. Ladóczki, J. Csontos, and B. Kornis. See also: Rolik, Z.; Szegedy, L.; Ladjánszki, I.; Ladóczki, B.; Kállay, M. *J. Chem. Phys.* **2013**, *139*, 094105 as well as www.mrcc.hu.
(62) Kállay, M. *J. Chem. Phys.* **2014**, *141*, 244113.
(63) Heßelmann, A. *Phys. Rev. A* **2012**, *85*, 012517.
(64) Mezei, P. D.; Csonka, G. I.; Ruzsinszky, A.; Sun, J. *J. Chem. Theory Comput.* **2015**, *11*, 360−371.
(65) Ren, X.; Tkatchenko, A.; Rinke, P.; Scheffler, M. *Phys. Rev. Lett.* **2011**, *106*, 16−19.
(66) Csonka, G. I.; Kaminsky, J. *J. Chem. Theory Comput.* **2011**, *7*, 988−997.
(67) Mezei, P. D.; Csonka, G. I.; Ruzsinszky, A. Submitted.
(68) Halkier, A.; Helgaker, T.; Jørgensen, P.; Klopper, W.; Koch, H.; Olsen, J.; Wilson, A. K. *Chem. Phys. Lett.* **1998**, *286*, 243−252.
(69) Heßelmann, A. *Top. Curr. Chem.* **2014**, *11*, 13−35.
(70) Wu, Q.; Yang, W. *J. Chem. Phys.* **2002**, *116*, 515−524.
(71) Chu, X.; Dalgarno, A. *J. Chem. Phys.* **2004**, *121*, 4083−4088.

DOI: 10.1021/acs.jctc.5b00223
J. Chem. Theory Comput. 2015, 11, 2879−2888